Drought indices of water demand and supply, soil moisture, vegetation, and its impact on LULCC in continental Chile

Francisco Zambrano[a,1,*]

[a] *Universidad Mayor, Hémera Centro de Observación de la Tierra, Facultad de Ciencias, Escuela de Ingeniería en Medio Ambiente y Sustentabilidad, Santiago, Chile, 7500994*

Abstract

Human-induced greenhouse gas emissions have increased the frequency and/or intensity of weather and climate extremes. Central Chile has been affected by a persistent drought which is impacting the hydrological system and vegetation development. The region has been the focus of research studies due to the diminishing water supply, this persistent period of water scarcity has been defined as a "mega drought". Nevertheless, our results evidence that the water deficit has expanded beyond. Our goal is to analyze the impact of drought, measured by drought indices of water supply/demand and vegetation status, in the LULCC (land use land cover change) over continental Chile. For the analysis, continental Chile was divided into five zones according to a latitudinal gradient: "Norte Grande", "Norte Chico", "Zona Central", "Zona Sur", and "Zona Austral". We used monthly climatic re-analysis variables for precipitation, temperature and soil moisture for 1981-2023 from ERA5-Land; and MODIS (Moderate-Resolution Imaging Spectroradiometer) product MCD12Q1 for land cover for 2001-2021, and the NDVI vegetation index from product MOD13A2 collection 6.1 for 2000-2023, both from collection 6.1. We estimated atmospheric evaporative demand (AED) by combining the Hargreaves-Samani equation with the ERA5-Land temperature. We derived the drought indices SPI (Standardized Precipitation Index), SPEI (Standardized Precipitation Evapotranspiration Index), EDDI (Evaporative Demand Drought Index), SSI (standardized anomaly of cumulative soil moisture), and the zcNDVI (standardized anomaly of cumulative NDVI). These indices were calculated for time scales of 1, 3, 6, 12, 24, and 36 months, except for zcNDVI (1, 3, and 6 months). We analyzed the temporal correlation of SPI, SPEI, EDDI, and SSI with zcNDVI to have insights into the impact of water supply and demand on vegetation. Our results showed that LULCC had an increasing trend of 412 [km2yr−1] of forest expansion in the "Zona Sur", together with a decreasing trend of 24 [km2yr−1] of cropland contraction in the "Zona Central" meanwhile the "Zona Sur" showed an increase of 31 [km2yr−1], and a contraction of 80 [km2yr−1] of bare soil in the "Zona Austral". The EDDI was the less correlated index for the five macro zones and the five types of land cover, showing that the temperature in Chile has little impact on vegetation. Higher r-squared values, between 0.5 and 0.8, were obtained at "Norte Chico" and "Zona Central" for the land cover types of savanna, shrubland, grassland, and croplands for the indices SPEI and SSI at time scales of 12 and 24 months. The forest type reaches a r-squared of ~0.5 for SSI of 12 months. The results indicate that the "Norte Chico" and "Zona Central" are the most sensitive regions to water supply deficits longer than a year, potentially explained by a low capacity of water storage in those zones that should be further investigated.

Keywords: drought, land cover change, satellite

*Corresponding author

Email address: francisco.zambrano@umayor.cl (Francisco Zambrano)

[1] This is the first author footnote.

1. Introduction

The sixth assessment report (AR6) of the IPCC [1] indicates that human-induced greenhouse gas emissions have increased the frequency and/or intensity of some weather and climate extremes, and the evidence has been strengthened since AR5 [2]. There is high confidence that increasing global warming can expand the land area affected by increasing drought frequency and severity [3]. Furthermore, drought increases tree mortality and triggers changes in land cover and, consequently, land use, thus impacting ecosystems [4]. Nevertheless, there is a lack of understanding of how the alteration in water supply and demand is affecting land cover transformations.

Precipitation is the primary driver of drought and is intensified by temperature [5]. Drought impacts soil moisture, hydrological regimes, and vegetation productivity. Initially, drought was commonly classified as meteorological, hydrological, and agricultural [6]. Lately, [7] and [8] have given an updated definition of drought for the Anthropocene, suggesting that it should be considered the feedback of humans' decisions and activities that drives the anthropogenic drought. Even though it has been argued that those definitions do not fully address the ecological dimensions of drought. [4] proposed the ecological drought definition as *"an episodic deficit in water availability that drives ecosystems beyond thresholds of vulnerability, impacts ecosystem services, and triggers feedback in natural and/or human systems"*. Moreover, many ecological studies have misinterpreted how to characterize drought, for example, sometimes considering "dry" conditions as "drought" [9]. On the other hand, the AR6 [1] states that even if global warming is stabilized at 1.5°–2°C, many parts of the world will be impacted by more severe agricultural and ecological droughts. Then, there is a challenge in conducting drought research, especially to evaluate its impact on ecosystems.

Chile has been facing a persistent rainfall deficit for more than a decade [10], which has impacted vegetation development [11] and the hydrological system [12]. Current drought conditions have affected crop productivity [13, 14], forest development [15, 16], forest fire occurrence [17], land cover change [18], water supply in watersheds [19], and have had economic impacts [20]. In 2019–2020, the drought severity reached an extreme condition in Central Chile (30–34°S) not seen for at least 40 years, and the evidence indicates that the impact is transversal to the land cover classes of forest, grassland, and cropland [11]. The prolonged lack of precipitation in Central Chile is producing changes in ecosystem dynamics that must be studied.

For the spatiotemporal assessment of drought impact (i.e., by water supply and demand) on land cover changes, we need climatic realiable variables such as precipitation, temperature, soil moisture, land cover, and vegetation status. For developing countries like Chile, the weather networks present several disadvantages, such as gaps, a short history, and low-quality data. Reanalysis data, as the ERA5-Land (ERA5L) [21] provides hourly climatic information (precipitation, temperature, and soil moisture) without gaps since 1950 with global extension. ERA5L has already been used for drought assessment using the Standardized Precipitation-Evapotranspiration Index (SPEI) [22] and for flash drought [23] by analyzing soil mositure and evapotranspiration. On the other hand, satellite remote sensing [24, 25] is the primary method to evaluate how drought impacts vegetation dynamics. Vegetation drought indices (VDI) are commonly used as proxies of productivity [26, 27], which can be derived from the MODIS (Moderate-Resolution Imaging Spectroradiometer). Besides, land use and land cover (LULC) change can be driven by drought [28, 29]. To analyze these changes, multiple LULC products exist [30], one of those that provides time series since 2001 is the MCD12Q1 [31] from MODIS. The variation in water supply and demand is finally reflected in the total water storage (TWS). The TWS can be retrieved by the Gravity Recovery and Climate Experiment (GRACE), which allows analyzing water availability changes at coarse resolution [32, 33]. We can use climatic reanalysis (ERA5L) and vegetation data (MODIS) to derive drought indices of supply (i.e., precipitation) and demand (i.e., temperature) and thus evaluate the impact of drought on LULC changes. Further, the TWS can be assessed with regard to the changes in water supply and demand to gain insight into the impact on water storage.

To evaluate meteorological drought (i.e., water supply), the World Meteorological Organization (WMO; [34]) recommends the Standardized Precipitation Index (SPI; [35]), a multiscalar drought index that allows to monitor precipitation deficits from short- to long-term. Following the same approach, [36] incorporates into the SPI the effect of temperature through the use of potential evapotranspiration, thus proposing the SPEI (Standardized Precipitation Evapotranspiration Index). Similarly, to evaluate solely the evaporative demand driven by temperature, [37] and [38] came up with the Evaporative Demand Drought Index (EDDI). For vegetation, in a similar manner as the SPI, SPEI and EDDI; [14] proposed the zcNDVI, a standardized anomaly of the cumulative Normalized Difference Vegetation Index (NDVI), which could be acumulated over the growing season or any period (e.g., months), resulting in a multiscalar drought index. For soil moisture, several drought indices exist, such as the Soil Moisture Deficit Index (SDMI) a normalized index [39] and the Soil Moisture Agricultural Drought Index (SMADI) [40] which is a normalized index using vegetation, land surface temperature, and a vegetation condition index (VCI, [41]). From TWS, we can estimate the standardized terrestrial water storage index (STI) [42], a standardized anomaly that follows the methodology of the SPI, SPEI, EDDI, and zcNDVI. Thereby, we have drought indices for water supply, demand, and storage, which can help to make a comprehensive assessment of drought.

In this research, we present the raster dataset DDS4Chl, which provides climate variables and drought indices of water demand and supply and vegetation productivity for continental Chile since 1981 at a monthly frequency. Those were gathered from the earth observation products ERA5-Land and MODIS. Then, we used DDS4Chl to analyze the impact of drought on different types of land cover classes in continental Chile. The specific objectives of the study are: i) to analyze the trend on multi-scalar drought indices for water demand and supply, soil moisture, and vegetation productivity for 1981–2023/2001–2023; ii) to evaluate LULC change for 2001–2021 and its relation to drought indices; iii) to analyze the relationship of a proxy of vegetation productivity (zcNDVI) with drought indices of water demand and supply and soil moisture; and iv) to assess if the observed changes in the drought indices are linked to TWS.

2. Study area

Continetal Chile has a diverse climate condition from north to south and east to west [43] (Figure 1), which determines its great ecosystem diversity (Figure 2). The Andes Mountains are a main factor in latitudinal variation [44]. To describe the climate and ecosystem of Chile, we use the Koppen-Geiger release by [45] and the landcover type persistance of 80% of times for 2001–2022, from the IGBP classification scheme [31] (see Section 3.5). "Norte Grande" and "Norte Chico" predominate in an arid desert climate with hot (Bwh) and cold (Bwk) temperatures. At the south of "Norte Chico," the climate changes to an arid steppe with cold temperatures (Bsk). Mainly, the land is barren, with a minor surface of vegetation types such as shrubland and grassland. In the zones "Centro" and the north half of "Sur," the main climate is Mediterranean, with warmer to hot summers (Csa and Csb). In "Centro," there is a major proportion (~50%) of chilean matorral (shrubland and savanna), followed by grassland (~16%), forest (8%), and croplands (5%). The south part of "Centro" and the north part of "Austral" are dominated by an Oceanic climate (Cfb). Those zones are high in forest and grassland. The southern part of the country has a tundra climate, and in Patagonia, it is a cold semi-arid area with an extended surface of grassland.

3. Materials and Methods

3.1. Software and packages used

For the downloading, processing, and analysis of the spatio-temporal data, we used the open source software for statistical computing and graphics, `R` [46]. For downloading ERA5-Land, we used the `{ecmwfr}` package [47]. For processing raster data, we used `{terra}` [48] and `{stars}` [49]. For managing vectorial data, we used `{sf}` [50]. For the calculation of AED, we used `{SPEI}` [51].

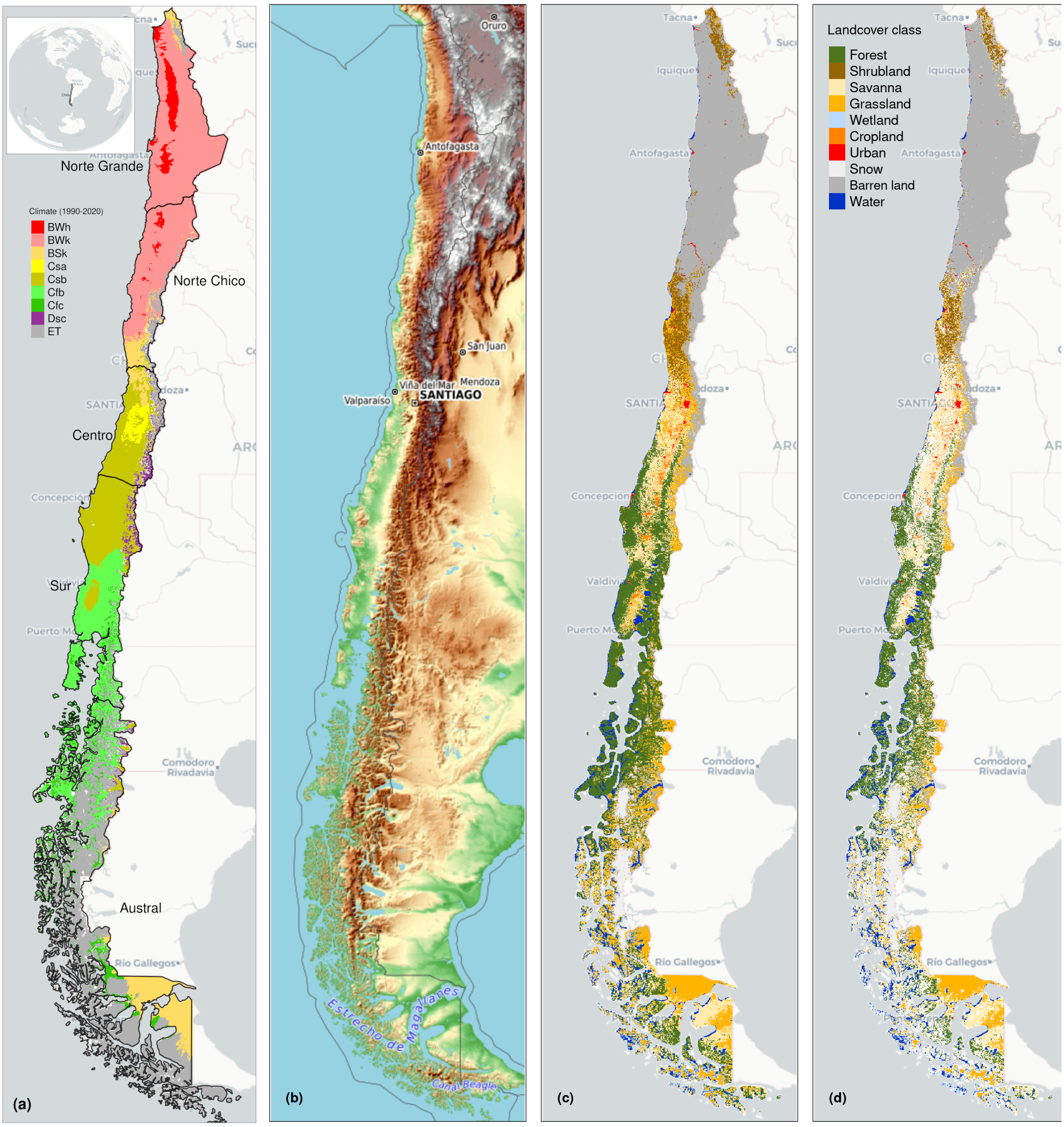

Figure 1: (a) Chile with the Koppen-Geiger climate classes and the five macrozones “Norte Grande”, “Norte Chico”, “Centro”, “Sur”, and “Austral”. (b) Topography reference map. (c) Land cover classes for 2022. (d) Persistent land cover classes (> 80%) for 2001-2022

3.2. Data

3.2.1. Earth observation data

For water supply and demand variables, we used ERA5-Land [21], a reanalys dataset that provides the evolution of land variables since 1950. It has a spatial resolution of 0.1°, hourly frequency, and global coverage. We selected the variables for total precipitation, 2 meter temperature maximum and minimum, and volumetric soil water layers between 0 and 100cm of depth (layer 1 to layer 3). The data was downloaded using the Copernicus Climate Data Store (CDS) Application Program Interface (API) implemented in `{ecmfwr}` [47].

To derive a proxy of vegetation productivity, we used the product MOD13A3 collection 6.1 from MODIS [52]. It provides vegetation indices (NDVI and EVI) at 1km of spatial resolution and monthly frequency. The MOD13A3.061 and MCD12Q1.061 were retrieved from the online Data Pool, courtesy of the NASA EOSDIS Land Processes Distributed Active Archive Center (LP DAAC), USGS Earth Resources Observation and Science (EROS) Center, Sioux Falls, South Dakota, https://lpdaa.usgs.gov/tools/data-pool/.

Table 1: Description of the earth observation data used

Product	Sub-product	Variable	Spatial Resolution	Period	Units	Short Name
ERA5-Land		Precipitation	0.1°	1981-2023	mm	P
		Maximum temperature			$°C$	T_{max}
		Minimum temperature			$°C$	T_{min}
		Volumetric Soil Water Content at 1m			$m3/m3$	SM
ERA5-Land*		Atmospheric Evaporative Demand	0.1°	1981-2023	mm	AED
MODIS	MOD13A3.061	Normalized Difference Vegetation Index	1 km	2000-2023		NDVI
	MCD12Q1.061	Landcover IGBP scheme		2001-2022		Landcover

*Derived from ERA5-Land with Eq. 1.

3.2.2. in-situ data

3.3. Drought Indices

We derived the drought indices of water supply and demand, soil moisture from the ERA5-Land dataset, and vegetation from the MODIS product, all at monthly frequency.

For the indices EDDI and SPEI that use water demand, first we have to calculate the AED. For this, we used the method of Hargreaves [53]:

$$AED = 0.0023 \cdot Ra \cdot (T + 17.8) \cdot (T_{max} - T_{min})^{0.5} \tag{1}$$

where Ra $(MJ\, m^2\, day^{-1})$ is extraterrestrial radiation; T, T_{max}, and T_{min} are mean, maximum, and minimum temperature ($°C$). We calculate the centroid coordinates per pixel and use the latitude to estimate Ra.

To evaluate water demand, we chose the $EDDI$ [37, 38] index, which uses the AED. For supply, we used the index recommended by the World Meteorological Organization (WMO) for monitoring drought, the SPI [35]. We calculated the SPEI, which used a balance between P and AED, in this case, an auxiliary variable $D = P - AED$ is used. In this study, we used the SSI (standardized soil moisture index at 1 m) [54, 55], which uses SM. Finally, for the proxy of productivity, $zcNDVI$, we used the NDVI. Before using the NDVI, it was smoothed following the procedure described in [14] and [13].

All the indices are multi-scalar and were calculated for time scales of 1, 3, 6, 12, 24, and 36 months, except for zcNDVI, which was calculated for 6 months. The goal is to be able to evaluate short- and long-term droughts in water demand and supply and soil moisture. This is particularly important for central Chile because it has suffered from a prolonged decrease in precipitation for more than 12 years [56, 12, 10].

To calculate the drought indices, first we must calculate the accumulation of the variable. In this case, for generalization purposes, we will use V, referring to P, AED, D, $NDVI$, and SM (Table 1). We cumulated each V over the time series of n values, and for the time scales s:

$$A_{si} = \sum_{i=n-s-i+2}^{n-i+1} V_i \; \forall \, i \geq n-s+1 \tag{2}$$

It corresponds to a moving window (convolution) that sums the variable for s starting for the last month n until the month, which could sum for s months (n-s+1). Once the variable is cumulated over time for the scale s, we used a nonparametric approach following [37] to derive the drought indices. Thus, the empirically derived probabilities are obtained through an inverse normal approximation [57]. Then, we used the empirical Tukey plotting position [58] over A_i to derive the $P(A_i)$ probabilities across a period of interest:

$$P(A_i) = \frac{i-0.33}{n+0.33'} \tag{3}$$

The drought indices SPI, $SPEI$, $EDDI$, SSI, and $zcNDVI$ are obtained following the inverse normal approximation:

$$DI(A_i) = W - \frac{C_0 + C_1 \cdot W + c_2 \cdot W^2}{1 + d_1 \cdot W + d_2 \cdot W^2 + d_3 \cdot W^3} \tag{4}$$

DI is referring to the drought index calculated for the variable V. The values for the constats are: $C_0 = 2.515517$, $C_1 = 0.802853$, $C_2 = 0.010328$, $d_1 = 1.432788$, $d_2 = 0.189269$, and $d3 = 0.001308$. For $P(A) \leq 0.5$, W=$\sqrt{-2 \cdot ln(P(A_i))}$, and for $P(A_i) > 0.5$, replace $P(A_i)$ with $1 - P(A_i)$ and reverse the sign of $DI(A_i)$.

3.4. Trend of drought indices for water demand and supply, soil moisture, and vegetation productivity

To estimate if there are significant positive or negative trends for the drought indices, we used the non-parametric test of Mann-Kendall [59]. To determine the magnitude of the trend, we used Sen's slope [60]. One of the advantages of applying this methodology is that the Sen's slope is not affected by outliers as regular regression does. We applied both to the five indices at the six time scales from 1981 to 2023 and indices SPI, EDDI, SPEI, and SSI, and from 2000 to 2023 in the case of zcNDVI.

[61] made a global analysis of the drought's severity trend using SPI, SPEI, and the Standardized Evapotranspiration Deficit Index (SEDI; [62]) to evaluate AED. They indicate that the increase in hydrological drought has been due to anthropogenic effects rather than climate change. This is because the global increase in AED does not explain the change in the spatial pattern of hydrological drought. Also, they state that *"the increase in hydrological droughts has been primarily observed in regions with high water demand and land cover change"*. We will contrast this hypothesis with what is occurring in Chile. To achieve this, we will use the landcover class type that remain more than 80% of types for 2001-2022, and use this as a mask, where there are low changes, to evaluate the trend on zcNDVI.

3.5. LULC change for 2001-2022 and its relation with water supply and demand, and soil moisture

To analyze the LULCC, we use the IGBP scheme from the MCD12Q1 collection 6.1 from MODIS. This product has a yearly frequency from 2011 to 2022. The IGBP defines 17 classes; from these, we regrouped into ten macroclasses for forest, schrublands, savannas, grasslands, wetlands, croplands, urban, snow and ice, barren, and water bodies. Then, we calculated the surface ocuppied per landcover class into each macrozone

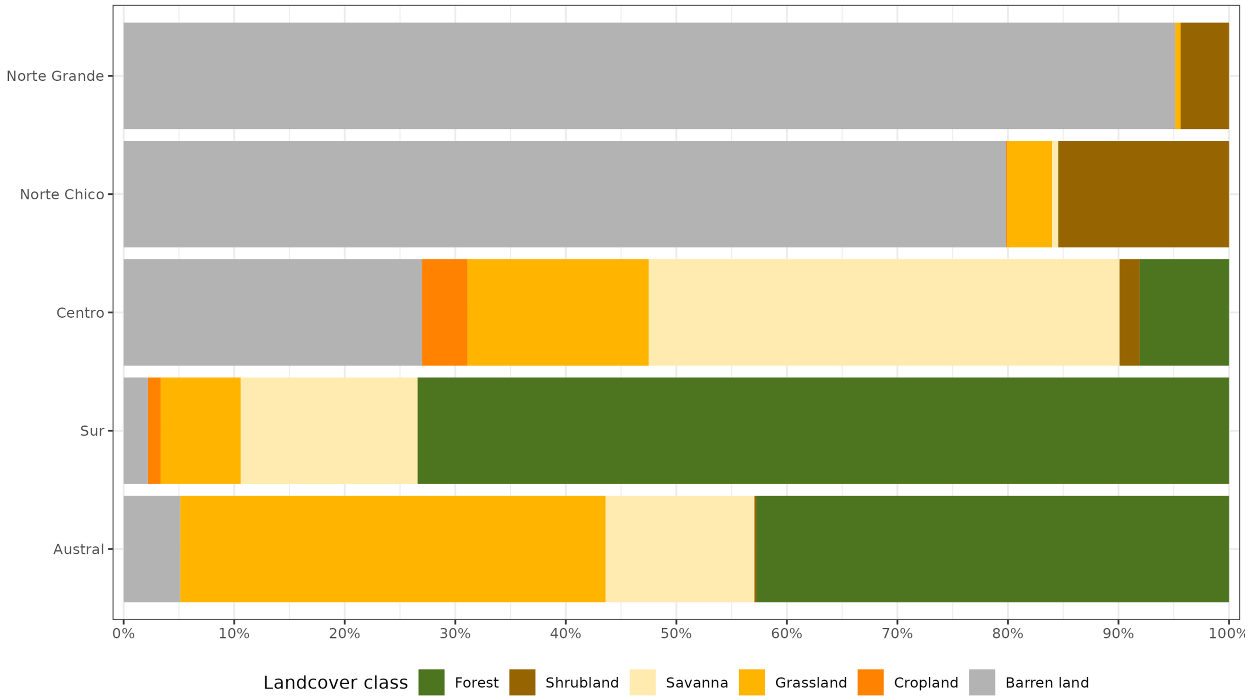

Figure 2: Proportion of land cover class from the persistent land cover for 2001-2022 (>80%) per macrozone

("Norte Grande" to "Austral") per year. To determine the trend of change we used the Sen' slope [60] over the surface per year.

We calculated a raster mask considering the classes that remains more than 80% of years (2001-2022), which allow us to identify the areas with no landcover change for the macroclasses. Figure 2 shows the summary of proportion of surface per landcover class and macrozone, derived from the mask over continental Chile.

We will explore if the trend in landcover classess is associated to trend of the drought indices. For this we will use the regularizations techniques of Lasso [63] and Ridge regressión [64]. Also, we will test random forest for this purpose [65].

3.6. Impact for water supply and demand, and soil moisture in vegetation productivity within landcover types

The aim of this section is to analyze the drought indices of water demand and supply and soil moisture against vegetation to address: i) if short- or long-term time scales are most important in impacting vegetation through Chile; and ii) the strength of the correlation for the variable and the time scale. Then, we will summarize for each landcover class and macrozone. Thus, we will be able to advance in understanding how climate is affecting vegetation, considering the impact on the five macroclasses: forest, cropland, grassland, savanna, and shrubland.

To assess how water demand and supply and soil moisture are related to vegetation productivity (zcNDVI), we analyze the linear correlation between the indices SPI, SPEI, EDDI, and SSI for 1, 3, 6, 12, 24, and 36-month time scales against zcNDVI. We followed a similar approach to that used by [66] when using the SPI for meteorological drought against the cumulative FAPAR (Fraction of Absorbed Photosynthetically Active Radiation) as a proxy for vegetation productivity. We made a pixel-to-pixel linear correlation analysis per index. First, we calculate the Pearson coefficient of correlation for the six time scales and let the time scale that reaches the maximum correlation be significant ($p < 0.05$). Then, we extracted the Pearson correlation value corresponding to the time scales that reached the maximum value. Thus, we derived two raster maps per index, the first with the time scales and the second with the correlation value.

3.7. Validation of ERA5-Land variables

4. Results

4.1. Trend of drought indices for water demand/supply, soil moisture, and vegetation productivity

Regarding vegetation productivity, there is a negative trend on zcNDVI in the central part of the country ("norte chico" and "zona central") (Figure 3). Indicating either a reduction of vegetation surface, biomass, or status. It reached its lowest values during the year 2020, mostly on the "zona central." There are other negative trends in small areas in "norte grande" and "zona asutral."

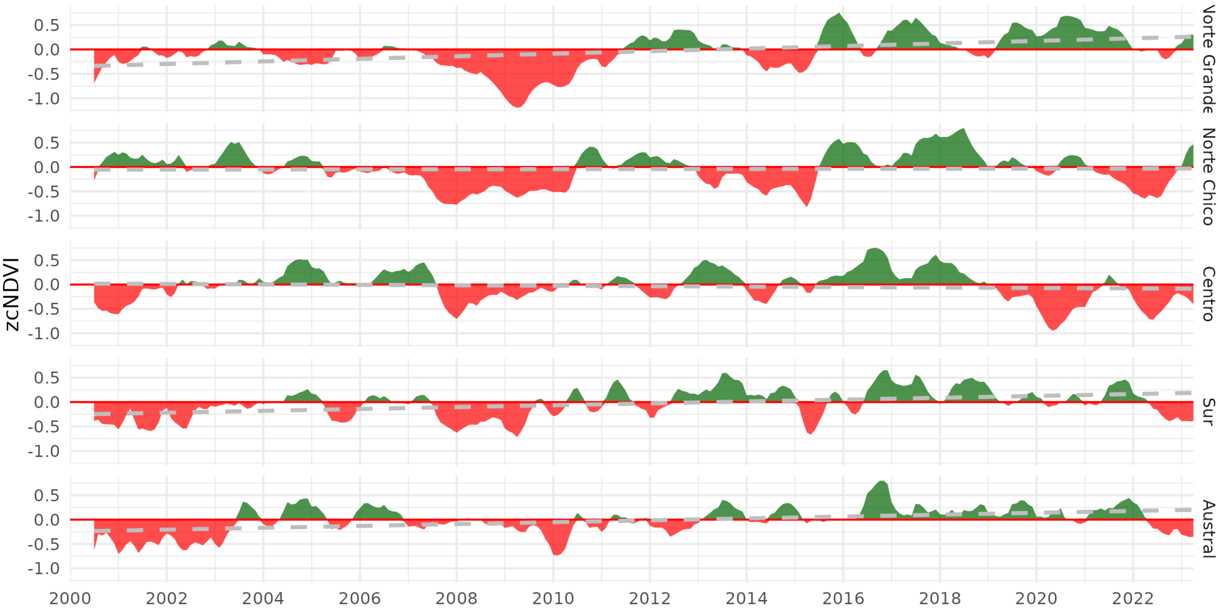

Figure 3: (a) Map of the linear trend of the index zcNDVI-6 for 2001–2023. Greener colors indicate a positive trend and an increase in vegetation development; reder colors correspond to a negative trend and a decrease in vegetation development. (b) Temporal variation of zcNDVI-6 aggregated at macrozone level within continental Chile. Each horizontal panel corresponds to a macrozone from 'norte grande' to 'zona austral'.

Analyzing the water supply in the macrozones "norte chico," "central," and "sur," the SPI shows a decreasing trend that increases at longer time scales due to the prolonged reduction in precipitation. It reaches a trend of -0.056 (z-score) per decade (Figure 4) for time scales of 36 months. In the case of water demand, we analyze the EDDI. It shows a positive trend, caused by an increase in AED. The trend on EDDI reaches a maximum of 0.053 per decade in the macrozones "norte grande" and "norte chico" (**?@fig-trendEDDI**). The behavior is similar to SPI, having close trends with opposite signs. Nevertheless, the spatial patterns are different. The maximum trend for SPI-36 is in "norte chico" and "zona central." For EDDI-36, the maximum trend is from "northe grande" to "zona central."

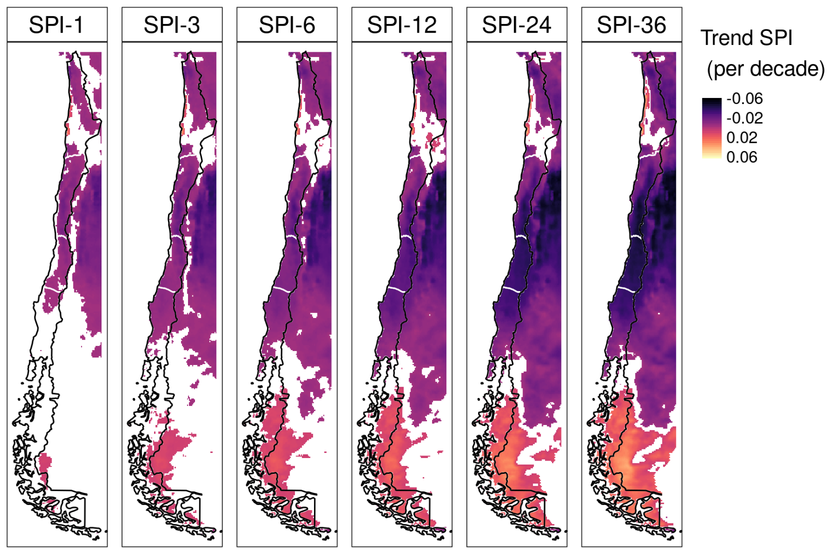

(a) SPI (Standardized Precipitation Index)

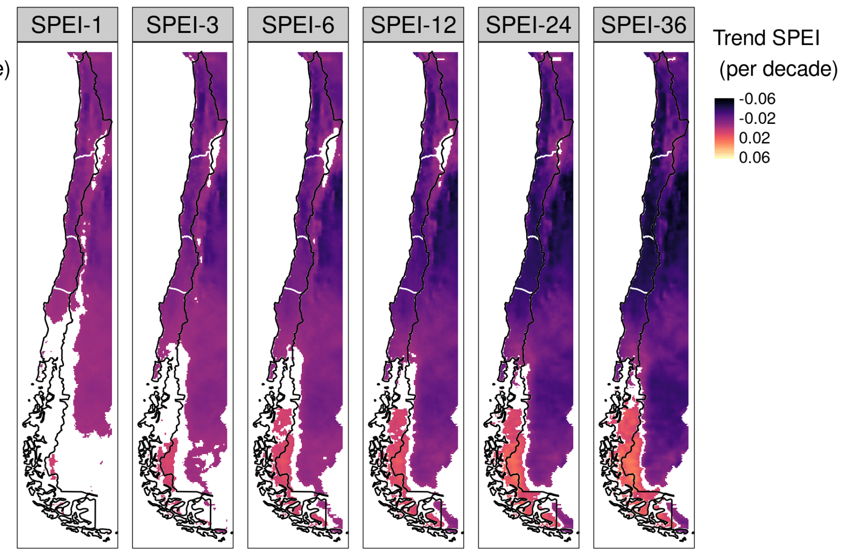

(b) SPEI (Standardized Precipitation Evapotranspiration Index)

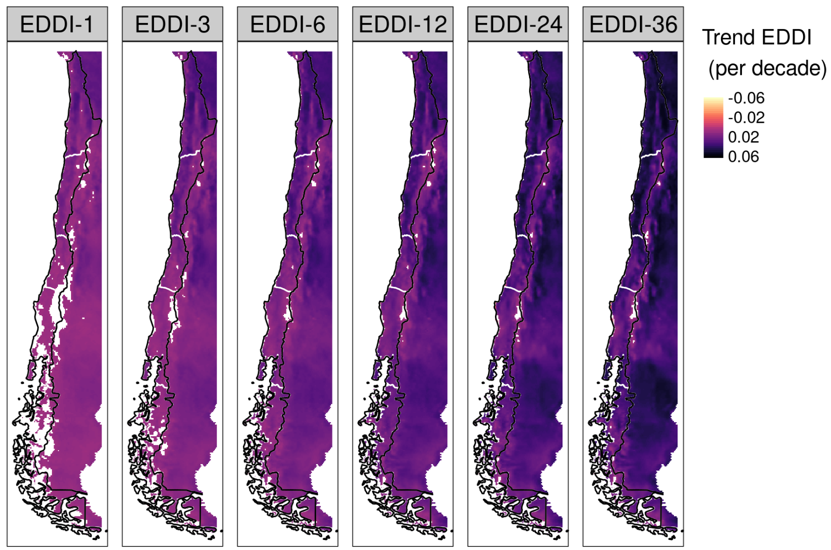

(c) EDDI (Evaporative Demand Drought Index)

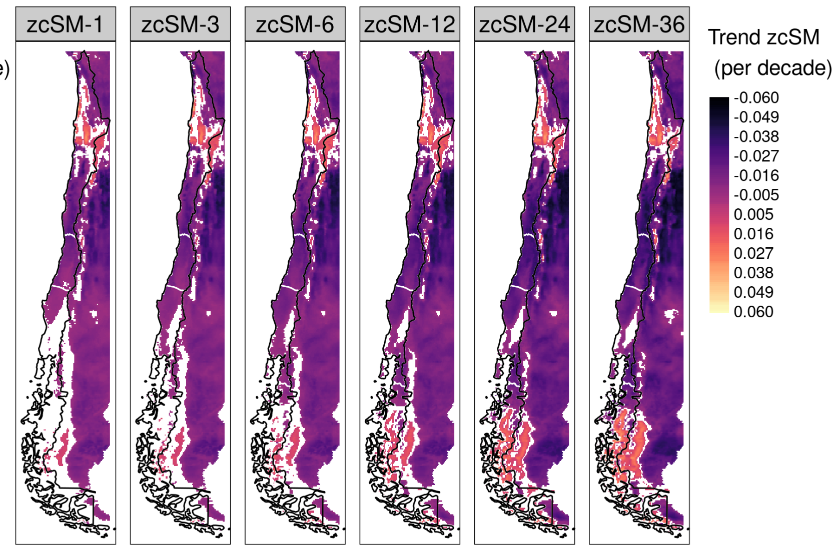

(d) SSMI (Standardized Soil Moisture Index)

Figure 4: Linear trend of the drought index (*) at time scales of 1, 3, 6, 12, 24, and 36 months for 1981-2023

The correlation between zcNDVI-6 and drought indices shows that time scales higher than six months are predominant over continental Chile in explaining vegetation variability (Figure 5). Pearson correlations between 0.6 and 0.9 are concentrated in the "norte chico" and "zona central" for SPI and SPEI. Soil moisture reached a correlation of 0.6–0.9 that extended north and south with respect to SPI.

4.2. Impact for water supply and demand, and soil moisture in vegetation productivity

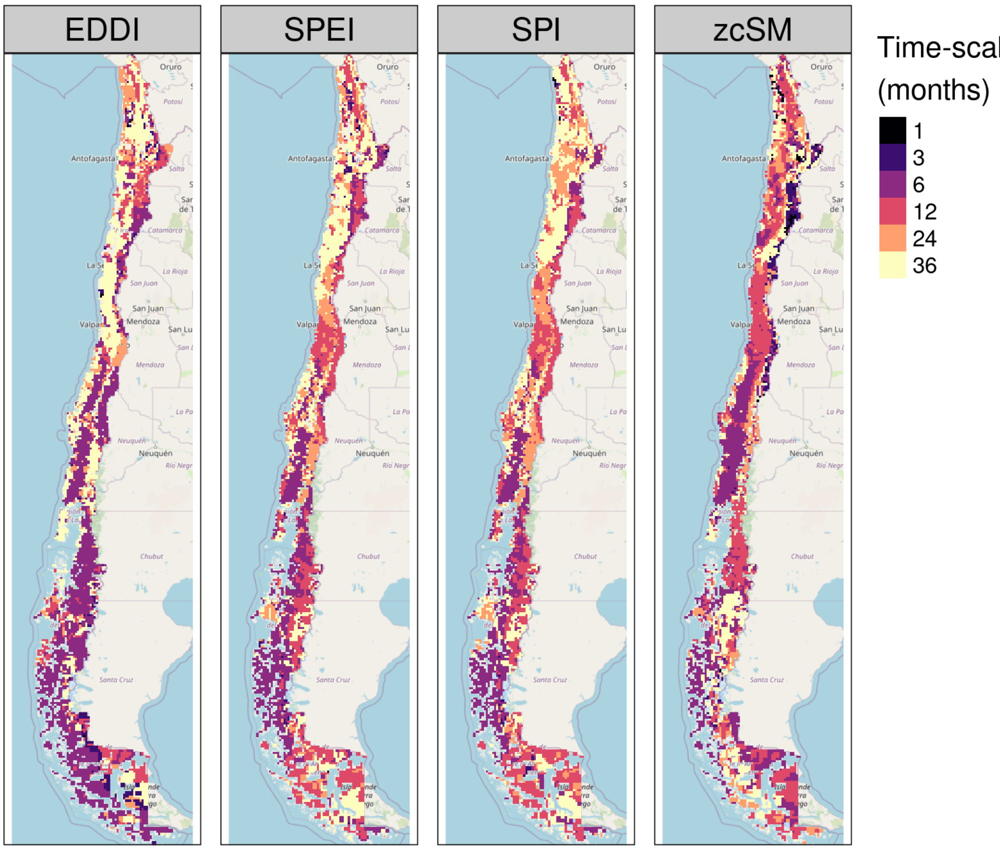

Figure 5: Time scales per drought index that reach the maximum coefficient of determination

4.3. LULC change for 2001-2022 and its relation with water supply and demand, and soil moisture

4.4. Total water storage (TWS) and drought indices

4.5. Validation of ERA5-Land variables

5. Discussion

6. Conclusion

References

[1] K. Calvin, D. Dasgupta, G. Krinner, A. Mukherji, P. W. Thorne, C. Trisos, J. Romero, P. Aldunce, K. Barrett, G. Blanco, W. W. Cheung, S. Connors, F. Denton, A. Diongue-Niang, D. Dodman, M. Garschagen, O. Geden, B. Hayward, C. Jones, F. Jotzo, T. Krug, R. Lasco, Y.-Y. Lee, V. Masson-Delmotte, M. Meinshausen, K. Mintenbeck, A. Mokssit, F. E. Otto,

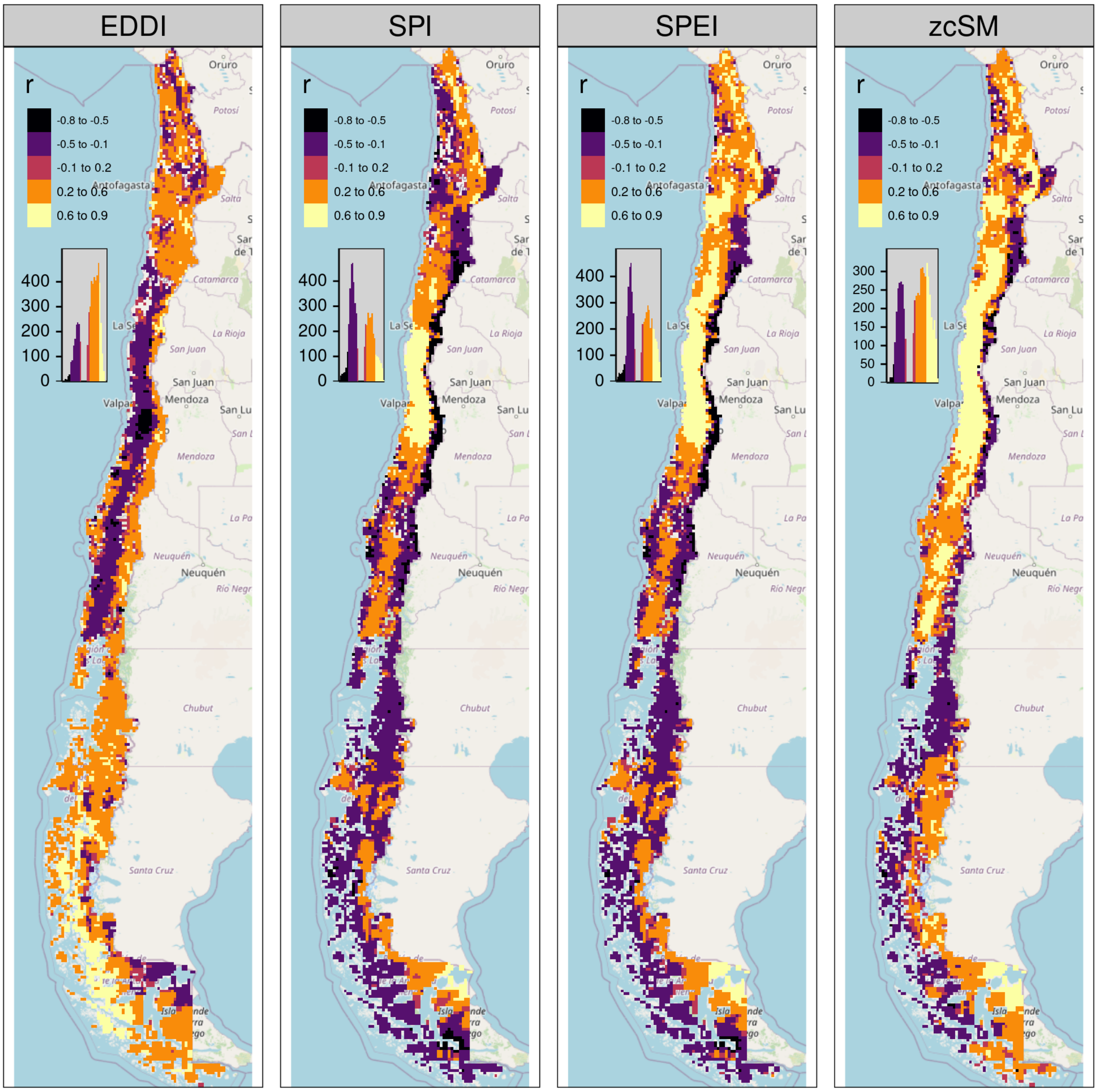

Figure 6: Pearson correlation value for the time scales and drought index that reach the maximum coefficient of determination

M. Pathak, A. Pirani, E. Poloczanska, H.-O. Pörtner, A. Revi, D. C. Roberts, J. Roy, A. C. Ruane, J. Skea, P. R. Shukla, R. Slade, A. Slangen, Y. Sokona, A. A. Sörensson, M. Tignor, D. Van Vuuren, Y.-M. Wei, H. Winkler, P. Zhai, Z. Zommers, J.-C. Hourcade, F. X. Johnson, S. Pachauri, N. P. Simpson, C. Singh, A. Thomas, E. Totin, P. Arias, M. Bustamante, I. Elgizouli, G. Flato, M. Howden, C. Méndez-Vallejo, J. J. Pereira, R. Pichs-Madruga, S. K. Rose, Y. Saheb, R. Sánchez Rodríguez, D. Ürge Vorsatz, C. Xiao, N. Yassaa, A. Alegría, K. Armour, B. Bednar-Friedl, K. Blok, G. Cissé, F. Dentener, S. Eriksen, E. Fischer, G. Garner, C. Guivarch, M. Haasnoot, G. Hansen, M. Hauser, E. Hawkins, T. Hermans, R. Kopp, N. Leprince-Ringuet, J. Lewis, D. Ley, C. Ludden, L. Niamir, Z. Nicholls, S. Some, S. Szopa, B. Trewin, K.-I. Van Der Wijst, G. Winter, M. Witting, A. Birt, M. Ha, J. Romero, J. Kim, E. F. Haites, Y. Jung, R. Stavins, A. Birt, M. Ha, D. J. A. Orendain, L. Ignon, S. Park, Y. Park, A. Reisinger, D. Cammaramo, A. Fischlin, J. S. Fuglestvedt, G. Hansen, C. Ludden, V. Masson-Delmotte, J. R. Matthews, K. Mintenbeck, A. Pirani, E. Poloczanska, N. Leprince-Ringuet, C. Péan, IPCC, 2023: Climate Change 2023: Synthesis Report. Contribution of Working Groups I, II and III to the Sixth Assessment Report of the Intergovernmental Panel on Climate Change [Core Writing Team, H.

Table 2: Value of linear change trend next to time-series plot of surface, per landcover class (IGBP MCD12Q1.006) for 2001-2019 through Central Chile. Red dots on the plots indicate the maximum and minimum surface

Trend of change [km^2 year^{-1}]

	Forest		Cropland		Grassland		Savanna		Shrubland		Barren land	
zone	x	y	x	y	x	y	x	y	x	y	x	y
Norte Grande						0.0				0.0		0.0
Norte Chico						0.0		−70.0		0.0		111.2
Centro		0.0		−22.4		83.2		−136.2		146.0		22.9
Sur		396.6		37.8		0.0		−318.8				0.0
Austral		0.0				0.0		172.1		−36.9		−93.2

Table 3

	Forest				Cropland				Grassland				Savanna				Shrubland			
macro	eddi	spi	spei	zcsm	eddi	spi	spei	zcsm	eddi	spi	spei	zcsm	eddi	spi	spei	zcsm	eddi	spi	spei	zcsm
norte grande									36	36	36	12	36	36	36	24	36	12	36	12
norte chico					36	36	12	12	36	36	24	12	36	24	24	12	36	36	24	12
centro		36	36	12	6	12	12	6	6	12	12	12	36	12	12	12	36	24	24	12
sur	36			6	6	6	6	6	6	6	6	12	6	6	6	6	6	12	12	24
austral	6	6			6	12	12	12	6	12	12	6	6	12		12	6	6	6	

r-squared 0.2 0.4 0.6

Lee and J. Romero (eds.)]. IPCC, Geneva, Switzerland., Tech. rep., Intergovernmental Panel on Climate Change (IPCC) (Jul. 2023).
URL https://www.ipcc.ch/report/ar6/syr/

[2] IPCC, Climate Change 2013: The Physical Science Basis. Contribution of Working Group I to the Fifth Assessment Report of the Intergovernmental Panel on Climate Change, Cambridge University Press, Cambridge, UK; New York, USA, 2013. doi:10.1017/CBO9781107415324.
URL www.climatechange2013.org

[3] X. a. A. M. a. B. W. a. D. C. a. L. A. a. G. S. a. I. I. a. K. J. a. L. S. a. O. F. a. P. I. a. S. M. a. V.-S. S. a. W. M. a. Z. . M.-D. B. a. V. a. O. Seneviratne, S and Zhang, Weather and Climate Extreme Events in a Changing Climate, Cambridge University Press. In Press., 2021, publication Title: Climate Change 2021: The Physical Science Basis. Contribution of Working Group I to the Sixth Assessment Report of the Intergovernmental Panel on Climate Change.

[4] S. D. Crausbay, A. R. Ramirez, S. L. Carter, M. S. Cross, K. R. Hall, D. J. Bathke, J. L. Betancourt, S. Colt, A. E. Cravens, M. S. Dalton, J. B. Dunham, L. E. Hay, M. J. Hayes, J. McEvoy, C. A. McNutt, M. A. Moritz, K. H. Nislow, N. Raheem, T. Sanford, Defining Ecological Drought for the Twenty-First Century, Bulletin of the American Meteorological Society 98 (12) (2017) 2543–2550, publisher: American Meteorological Society. doi:10.1175/BAMS-D-16-0292.1.
URL https://journals.ametsoc.org/view/journals/bams/98/12/bams-d-16-0292.1.xml

[5] L. Luo, D. Apps, S. Arcand, H. Xu, M. Pan, M. Hoerling, Contribution of temperature and precipitation anomalies to the California drought during 2012–2015, Geophysical Research Letters 44 (7) (2017) 3184–3192. doi:10.1002/2016GL072027.
URL https://agupubs.onlinelibrary.wiley.com/doi/10.1002/2016GL072027

[6] D. A. Wilhite, M. H. Glantz, Understanding: The drought phenomenon: The role of definitions, Water International 10 (3) (1985) 111–120. doi:10.1080/02508068508686328.
URL http://dx.doi.org/10.1080/02508068508686328

[7] A. F. Van Loon, T. Gleeson, J. Clark, A. I. Van Dijk, K. Stahl, J. Hannaford, G. Di Baldassarre, A. J. Teuling, L. M. Tallaksen, R. Uijlenhoet, D. M. Hannah, J. Sheffield, M. Svoboda, B. Verbeiren, T. Wagener, S. Rangecroft, N. Wanders, H. A. Van Lanen, Drought in the Anthropocene, Nature Geoscience 9 (2) (2016) 89–91. doi:10.1038/ngeo2646.

[8] A. AghaKouchak, A. Mirchi, K. Madani, G. Di Baldassarre, A. Nazemi, A. Alborzi, H. Anjileli, M. Azarderakhsh, F. Chiang, E. Hassanzadeh, L. S. Huning, I. Mallakpour, A. Martinez, O. Mazdiyasni, H. Moftakhari, H. Norouzi, M. Sadegh, D. Sadeqi, A. F. Van Loon, N. Wanders, Anthropogenic Drought: Definition, Challenges, and Opportunities,

Reviews of Geophysics 59 (2) (2021) e2019RG000683. doi:10.1029/2019RG000683.
URL https://agupubs.onlinelibrary.wiley.com/doi/10.1029/2019RG000683

[9] I. J. Slette, A. K. Post, M. Awad, T. Even, A. Punzalan, S. Williams, M. D. Smith, A. K. Knapp, How ecologists define drought, and why we should do better, Global Change Biology 25 (10) (2019) 3193–3200. doi:10.1111/gcb.14747.
URL https://onlinelibrary.wiley.com/doi/10.1111/gcb.14747

[10] R. Garreaud, C. Alvarez-Garreton, J. Barichivich, J. P. Boisier, D. Christie, M. Galleguillos, C. LeQuesne, J. McPhee, M. Zambrano-Bigiarini, The 2010-2015 mega drought in Central Chile: Impacts on regional hydroclimate and vegetation, Hydrology and Earth System Sciences Discussions 2017 (2017) 1–37. doi:10.5194/hess-2017-191.
URL http://www.hydrol-earth-syst-sci-discuss.net/hess-2017-191/

[11] F. Zambrano, Four decades of satellite data for agricultural drought monitoring throughout the growing season in Central Chile, in: R. M. Vijay P. Singh Deepak Jhajharia, R. Kumar (Eds.), Integrated Drought Management, Two Volume Set, CRC Press, 2023, p. 28.

[12] J. P. Boisier, C. Alvarez-Garreton, R. R. Cordero, A. Damiani, L. Gallardo, R. D. Garreaud, F. Lambert, C. Ramallo, M. Rojas, R. Rondanelli, Anthropogenic drying in central-southern Chile evidenced by long-term observations and climate model simulations, Elementa 6 (1) (2018) 74. doi:10.1525/elementa.328.
URL https://www.elementascience.org/article/10.1525/elementa.328/

[13] F. Zambrano, M. Lillo-Saavedra, K. Verbist, O. Lagos, Sixteen years of agricultural drought assessment of the biobío region in chile using a 250 m resolution vegetation condition index (VCI), Remote Sensing 8 (6) (2016) 1–20, publisher: Multidisciplinary Digital Publishing Institute. doi:10.3390/rs8060530.
URL http://www.mdpi.com/2072-4292/8/6/530

[14] F. Zambrano, A. Vrieling, A. Nelson, M. Meroni, T. Tadesse, Prediction of drought-induced reduction of agricultural productivity in Chile from MODIS, rainfall estimates, and climate oscillation indices, Remote Sensing of Environment 219 (2018) 15–30, publisher: Elsevier. doi:10.1016/j.rse.2018.10.006.
URL https://www.sciencedirect.com/science/article/pii/S0034425718304541

[15] A. Miranda, A. Lara, A. Altamirano, C. Di Bella, M. E. González, J. Julio Camarero, Forest browning trends in response to drought in a highly threatened mediterranean landscape of South America, Ecological Indicators 115 (2020) 106401. doi:10.1016/j.ecolind.2020.106401.
URL https://linkinghub.elsevier.com/retrieve/pii/S1470160X20303381

[16] A. Venegas-González, F. R. Juñent, A. G. Gutiérrez, M. T. Filho, Recent radial growth decline in response to increased drought conditions in the northernmost Nothofagus populations from South America, Forest Ecology and Management 409 (2018) 94–104. doi:10.1016/j.foreco.2017.11.006.
URL https://linkinghub.elsevier.com/retrieve/pii/S0378112717313993

[17] R. Urrutia-Jalabert, M. E. González, . González-Reyes, A. Lara, R. Garreaud, Climate variability and forest fires in central and south-central Chile, Ecosphere 9 (4) (2018) e02171. doi:10.1002/ecs2.2171.
URL https://esajournals.onlinelibrary.wiley.com/doi/10.1002/ecs2.2171

[18] I. Fuentes, R. Fuster, D. Avilés, W. Vervoort, Water scarcity in central Chile: the effect of climate and land cover changes on hydrologic resources, Hydrological Sciences Journal 66 (6) (2021) 1028–1044. doi:10.1080/02626667.2021.1903475.
URL https://www.tandfonline.com/doi/full/10.1080/02626667.2021.1903475

[19] C. Alvarez-Garreton, J. P. Boisier, R. Garreaud, J. Seibert, M. Vis, Progressive water deficits during multiyear droughts in basins with long hydrological memory in Chile, Hydrology and Earth System Sciences 25 (1) (2021) 429–446. doi:10.5194/hess-25-429-2021.
URL https://hess.copernicus.org/articles/25/429/2021/

[20] F. J. Fernández, F. Vásquez-Lavín, R. D. Ponce, R. Garreaud, F. Hernández, O. Link, F. Zambrano, M. Hanemann, The economics impacts of long-run droughts: Challenges, gaps, and way forward, Journal of Environmental Management 344 (2023) 118726. doi:10.1016/j.jenvman.2023.118726.
URL https://linkinghub.elsevier.com/retrieve/pii/S0301479723015141

[21] J. Muñoz-Sabater, E. Dutra, A. Agustí-Panareda, C. Albergel, G. Arduini, G. Balsamo, S. Boussetta, M. Choulga, S. Harrigan, H. Hersbach, B. Martens, D. G. Miralles, M. Piles, N. J. Rodríguez-Fernández, E. Zsoter, C. Buontempo, J.-N. Thépaut, ERA5-Land: a state-of-the-art global reanalysis dataset for land applications, Earth System Science Data 13 (9) (2021) 4349–4383. doi:10.5194/essd-13-4349-2021.
URL https://essd.copernicus.org/articles/13/4349/2021/

[22] M. Nouri, Drought Assessment Using Gridded Data Sources in Data-Poor Areas with Different Aridity Conditions, Water Resources Management 37 (11) (2023) 4327–4343. doi:10.1007/s11269-023-03555-4.
URL https://link.springer.com/10.1007/s11269-023-03555-4

[23] M. Wang, L. Menzel, S. Jiang, L. Ren, C.-Y. Xu, H. Cui, Evaluation of flash drought under the impact of heat wave events in southwestern Germany, Science of The Total Environment 904 (2023) 166815. doi:10.1016/j.scitotenv.2023.166815.
URL https://linkinghub.elsevier.com/retrieve/pii/S0048969723054402

[24] H. West, N. Quinn, M. Horswell, Remote sensing for drought monitoring \& impact assessment: Progress, past challenges and future opportunities, Remote Sensing of Environment 232, publisher: Elsevier Inc. (Oct. 2019). doi:10.1016/j.rse.2019.111291.

[25] A. AghaKouchak, A. Farahmand, F. S. Melton, J. Teixeira, M. C. Anderson, B. D. Wardlow, C. R. Hain, Remote sensing of drought: Progress, challenges and opportunities, Reviews of Geophysics 53 (2) (2015) 452–480. doi:10.1002/2014RG000456.
URL http://dx.doi.org/10.1002/2014RG000456.

[26] J. M. Paruelo, M. Texeira, L. Staiano, M. Mastrángelo, L. Amdan, F. Gallego, An integrative index of Ecosystem Services

provision based on remotely sensed data, Ecological Indicators 71 (2016) 145–154, publisher: Elsevier. doi:10.1016/J.ECOLIND.2016.06.054.
URL https://www.sciencedirect.com/science/article/pii/S1470160X16303843

[27] A. Schucknecht, M. Meroni, F. Kayitakire, A. Boureima, A. Schucknecht, M. Meroni, F. Kayitakire, A. Boureima, Phenology-Based Biomass Estimation to Support Rangeland Management in Semi-Arid Environments, Remote Sensing 9 (5) (2017) 463, publisher: Multidisciplinary Digital Publishing Institute. doi:10.3390/rs9050463.
URL http://www.mdpi.com/2072-4292/9/5/463

[28] H. T. Tran, J. B. Campbell, R. H. Wynne, Y. Shao, S. V. Phan, Drought and Human Impacts on Land Use and Land Cover Change in a Vietnamese Coastal Area, Remote Sensing 2019, Vol. 11, Page 333 11 (3) (2019) 333, publisher: Multidisciplinary Digital Publishing Institute. doi:10.3390/RS11030333.
URL https://www.mdpi.com/2072-4292/11/3/333/htm

[29] F. O. Akinyemi, Vegetation Trends, Drought Severity and Land Use-Land Cover Change during the Growing Season in Semi-Arid Contexts, Remote Sensing 2021, Vol. 13, Page 836 13 (5) (2021) 836, publisher: Multidisciplinary Digital Publishing Institute. doi:10.3390/RS13050836.
URL https://www.mdpi.com/2072-4292/13/5/836/htm

[30] G. Grekousis, G. Mountrakis, M. Kavouras, An overview of 21 global and 43 regional land-cover mapping products, International Journal of Remote Sensing 36 (21) (2015) 5309–5335. doi:10.1080/01431161.2015.1093195.
URL https://www.tandfonline.com/doi/full/10.1080/01431161.2015.1093195

[31] M. Friedl, D. Sulla-Menashe, MCD12Q1 MODIS/Terra+Aqua Land Cover Type Yearly L3 Global 500m SIN Grid V006 [Data set]. NASA EOSDIS Land Processes DAAC (2019). doi:10.5067/MODIS/MCD12Q1.006.

[32] M. Ahmed, M. Sultan, J. Wahr, E. Yan, The use of GRACE data to monitor natural and anthropogenic induced variations in water availability across Africa, Earth-Science Reviews 136 (2014) 289–300, publisher: Elsevier. doi:10.1016/J.EARSCIREV.2014.05.009.

[33] S. Ma, Q. Wu, J. Wang, S. Zhang, Temporal Evolution of Regional Drought Detected from GRACE TWSA and CCI SM in Yunnan Province, China, Remote Sensing 2017, Vol. 9, Page 1124 9 (11) (2017) 1124, publisher: Multidisciplinary Digital Publishing Institute. doi:10.3390/RS9111124.
URL https://www.mdpi.com/2072-4292/9/11/1124/htm

[34] WMO, M. Svoboda, M. Hayes, D. A. Wood, Standardized Precipitation Index User Guide, WMO, Geneva, 2012, series Title: WMO Publication Title: WMO-No. 1090 © Issue: 1090.
URL http://library.wmo.int/opac/index.php?lvl=notice_display&id=13682

[35] T. B. Mckee, N. J. Doesken, J. Kleist, The relationship of drought frequency and duration to time scales. In: Proceedings of the Ninth Conference on Applied Climatology., American Metereological Society (Boston) (1993) 179–184.

[36] S. M. Vicente-Serrano, S. Beguería, J. I. López-Moreno, A multiscalar drought index sensitive to global warming: The standardized precipitation evapotranspiration index, Journal of Climate 23 (7) (2010) 1696–1718. doi:10.1175/2009JCLI2909.1.
URL http://dx.doi.org/10.1175/2009JCLI2909.1

[37] M. T. Hobbins, A. Wood, D. J. McEvoy, J. L. Huntington, C. Morton, M. Anderson, C. Hain, The Evaporative Demand Drought Index. Part I: Linking Drought Evolution to Variations in Evaporative Demand, Journal of Hydrometeorology 17 (6) (2016) 1745–1761. doi:10.1175/JHM-D-15-0121.1.
URL http://journals.ametsoc.org/doi/10.1175/JHM-D-15-0121.1

[38] D. J. McEvoy, J. L. Huntington, M. T. Hobbins, A. Wood, C. Morton, M. Anderson, C. Hain, The Evaporative Demand Drought Index. Part II: CONUS-Wide Assessment against Common Drought Indicators, Journal of Hydrometeorology 17 (6) (2016) 1763–1779. doi:10.1175/JHM-D-15-0122.1.
URL http://journals.ametsoc.org/doi/10.1175/JHM-D-15-0122.1

[39] B. Narasimhan, R. Srinivasan, Development and evaluation of Soil Moisture Deficit Index (SMDI) and Evapotranspiration Deficit Index (ETDI) for agricultural drought monitoring, Agricultural and Forest Meteorology 133 (1-4) (2005) 69–88. doi:10.1016/j.agrformet.2005.07.012.
URL https://linkinghub.elsevier.com/retrieve/pii/S0168192305001565

[40] A. G. S. S. Souza, A. Ribeiro Neto, L. L. D. Souza, Soil moisture-based index for agricultural drought assessment: SMADI application in Pernambuco State-Brazil, Remote Sensing of Environment 252 (2021) 112124. doi:10.1016/j.rse.2020.112124.
URL https://linkinghub.elsevier.com/retrieve/pii/S0034425720304971

[41] F. N. Kogan, Application of vegetation index and brightness temperature for drought detection, Advances in Space Research 15 (11) (1995) 91–100. doi:10.1016/0273-1177(95)00079-T.

[42] A. Cui, J. Li, Q. Zhou, R. Zhu, H. Liu, G. Wu, Q. Li, Use of a multiscalar GRACE-based standardized terrestrial water storage index for assessing global hydrological droughts, Journal of Hydrology 603 (2021) 126871. doi:10.1016/j.jhydrol.2021.126871.
URL https://linkinghub.elsevier.com/retrieve/pii/S0022169421009215

[43] P. Aceituno, J. P. Boisier, R. Garreaud, R. Rondanelli, J. A. Rutllant, Climate and Weather in Chile, in: B. Fernández, J. Gironás (Eds.), Water Resources of Chile, Vol. 8, Springer International Publishing, Cham, 2021, pp. 7–29.
URL http://link.springer.com/10.1007/978-3-030-56901-3_2

[44] R. D. Garreaud, The Andes climate and weather, Advances in Geosciences 22 (2009) 3–11. doi:10.5194/adgeo-22-3-2009.
URL https://adgeo.copernicus.org/articles/22/3/2009/

[45] H. E. Beck, T. R. McVicar, N. Vergopolan, A. Berg, N. J. Lutsko, A. Dufour, Z. Zeng, X. Jiang, A. I. J. M. van Dijk, D. G. Miralles, High-resolution (1 km) Köppen-Geiger maps for 1901–2099 based on constrained CMIP6 projections, Scientific

Data 10 (1) (Oct. 2023). doi:10.1038/s41597-023-02549-6.
URL http://dx.doi.org/10.1038/s41597-023-02549-6

[46] R Core Team, R: A Language and Environment for Statistical Computing, R Foundation for Statistical Computing, Vienna, Austria, 2023.
URL https://www.R-project.org/

[47] K. Hufkens, R. Stauffer, E. Campitelli, The ecwmfr package: an interface to ECMWF API endpoints (2019).
URL https://bluegreen-labs.github.io/ecmwfr/

[48] R. J. Hijmans, terra: Spatial Data Analysis, 2023.
URL https://CRAN.R-project.org/package=terra

[49] E. Pebesma, R. Bivand, Spatial Data Science: With applications in R, Chapman and Hall/CRC, London, 2023.
URL https://r-spatial.org/book/

[50] E. Pebesma, Simple Features for R: Standardized Support for Spatial Vector Data, The R Journal 10 (1) (2018) 439–446. doi:10.32614/RJ-2018-009.
URL https://doi.org/10.32614/RJ-2018-009

[51] S. Beguería, S. M. Vicente-Serrano, SPEI: Calculation of the Standardized Precipitation-Evapotranspiration Index, 2023.
URL https://CRAN.R-project.org/package=SPEI

[52] K. Didan, MOD13Q1 MODIS/Terra Vegetation Indices 16-Day L3 Global 250m SIN Grid V006, Tech. rep., NASA EOSDIS Land Processes DAAC (2015). doi:http://dx.doi.org/10.5067/MODIS/MOD13Q1.006.

[53] G. H. Hargreaves, Defining and Using Reference Evapotranspiration, Journal of Irrigation and Drainage Engineering 120 (6) (1994) 1132–1139. doi:10.1061/(ASCE)0733-9437(1994)120:6(1132).
URL https://ascelibrary.org/doi/10.1061/%28ASCE%290733-9437%281994%29120%3A6%281132%29

[54] Z. Hao, A. AghaKouchak, Multivariate Standardized Drought Index: A parametric multi-index model, Advances in Water Resources 57 (2013) 12–18. doi:10.1016/j.advwatres.2013.03.009.
URL https://linkinghub.elsevier.com/retrieve/pii/S0309170813000493

[55] A. AghaKouchak, A baseline probabilistic drought forecasting framework using standardized soil moisture index: application to the 2012 United States drought, Hydrology and Earth System Sciences 18 (7) (2014) 2485–2492. doi:10.5194/hess-18-2485-2014.
URL https://hess.copernicus.org/articles/18/2485/2014/

[56] R. D. Garreaud, J. P. Boisier, R. Rondanelli, A. Montecinos, H. H. Sepúlveda, D. Veloso-Aguila, The Central Chile Mega Drought (2010–2018): A climate dynamics perspective, International Journal of Climatology 40 (1) (2020) 421–439. doi:10.1002/joc.6219.
URL https://rmets.onlinelibrary.wiley.com/doi/10.1002/joc.6219

[57] M. Abramowitz, I. A. Stegun, Handbook of mathematical functions with formulas, graphs, and mathematical tables, Vol. 55, US Government printing office, 1968.

[58] D. S. Wilks, Empirical distributions and exploratory data analysis, Statistical Methods in the Atmospheric Sciences 100 (2011).

[59] M. Kendall, Rank correlation methods (4th ed, 2d impression). Griffin, 1975.

[60] P. K. Sen, Estimates of the Regression Coefficient Based on Kendall's Tau, Journal of the American Statistical Association 63 (324) (1968) 1379–1389. doi:10.1080/01621459.1968.10480934.
URL http://www.tandfonline.com/doi/abs/10.1080/01621459.1968.10480934

[61] S. M. Vicente-Serrano, D. Peña-Angulo, S. Beguería, F. Domínguez-Castro, M. Tomás-Burguera, I. Noguera, L. Gimeno-Sotelo, A. El Kenawy, Global drought trends and future projections, Philosophical Transactions of the Royal Society A: Mathematical, Physical and Engineering Sciences 380 (2238) (2022) 20210285. doi:10.1098/rsta.2021.0285.
URL https://royalsocietypublishing.org/doi/10.1098/rsta.2021.0285

[62] S. M. Vicente-Serrano, D. G. Miralles, F. Domínguez-Castro, C. Azorin-Molina, A. El Kenawy, T. R. McVicar, M. Tomás-Burguera, S. Beguería, M. Maneta, M. Peña-Gallardo, Global Assessment of the Standardized Evapotranspiration Deficit Index (SEDI) for Drought Analysis and Monitoring, Journal of Climate 31 (14) (2018) 5371–5393. doi:10.1175/JCLI-D-17-0775.1.
URL https://journals.ametsoc.org/doi/10.1175/JCLI-D-17-0775.1

[63] R. Tibshirani, J. Bien, J. Friedman, T. Hastie, N. Simon, J. Taylor, R. J. Tibshirani, Strong rules for discarding predictors in lasso-type problems (Nov. 2010).
URL http://arxiv.org/abs/1011.2234

[64] A. E. Hoerl, R. W. Kennard, Ridge Regression: Biased Estimation for Nonorthogonal Problems, Technometrics 12 (1) (1970) 55–67. doi:10.1080/00401706.1970.10488634.
URL http://www.tandfonline.com/doi/abs/10.1080/00401706.1970.10488634

[65] T. K. Ho, Random decision forests, in: Proceedings of 3rd international conference on document analysis and recognition, Vol. 1, IEEE, 1995, pp. 278–282.

[66] M. Meroni, F. Rembold, D. Fasbender, A. Vrieling, Evaluation of the Standardized Precipitation Index as an early predictor of seasonal vegetation production anomalies in the Sahel, Remote Sensing Letters 8 (4) (2017) 301–310. doi:10.1080/2150704X.2016.1264020.
URL https://www.tandfonline.com/doi/full/10.1080/2150704X.2016.1264020